ÉCOLE POLYTECHNIQUE FÉDÉRALE DE LAUSANNE

Project in space technologies : SSA study for radio detection of objects in space

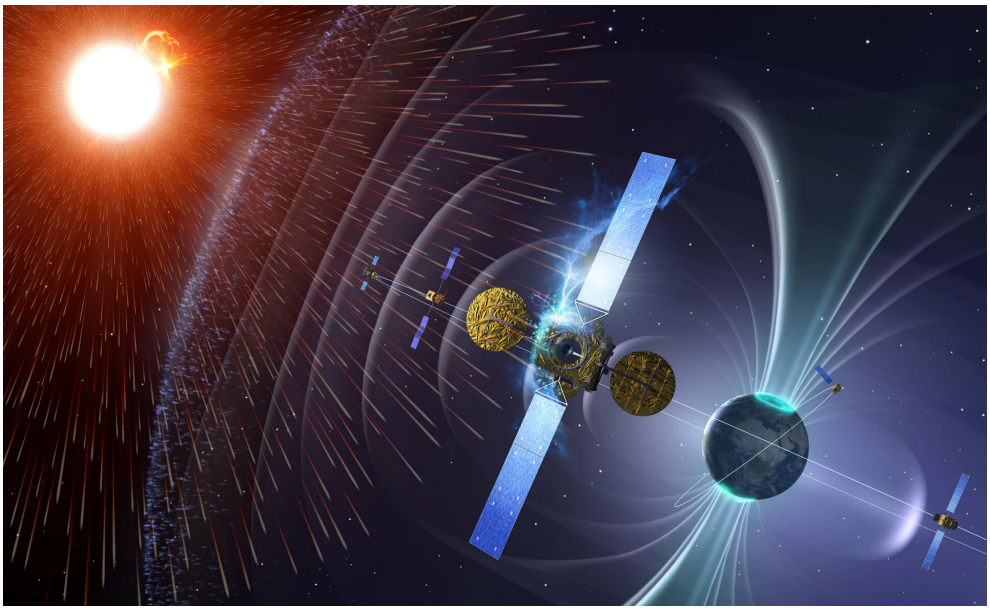

Falkenback Tanguy [Sciper : 350603]
Course : EE - 589
Teacher : Jean-Paul Kneib
Supervisor : Emma Elizabeth Tolley
Email : tanguy.falkenback@epfl.ch
June 3, 2022

EPFL

CONTENTS

I Introduction 4

II GRAVES 4
- II-A Overview . . . 4
  - II-A1 Situation . . . 4
  - II-A2 Principle . . . 4
- II-B Mathematical approach . . . 5
- II-C Block system . . . 7
  - II-C1 Antenna . . . 7
  - II-C2 Preamplifier . . . 7
  - II-C3 Transmission line . . . 8
  - II-C4 Band pass filter . . . 8
  - II-C5 Receiver . . . 8
  - II-C6 Program . . . 8

III FMCW 8
- III-A Overview . . . 8
- III-B Mathematical approach . . . 9
- III-C Block system . . . 10
  - III-C1 Modulator . . . 10
  - III-C2 Voltage Controlled Oscillator (VCO) . . . 10
  - III-C3 Splitter . . . 10
  - III-C4 Mixer . . . 10
  - III-C5 Computer . . . 11

IV Passive detection 12
- IV-A Overview . . . 12
- IV-B Mathematical approach . . . 12
- IV-C Block system . . . 14

V Angular resolution 14

VI Recommendation 15

VII Conclusion 15

References 16

LIST OF FIGURES

1 Map of the situation of GRAVES in France. The emission site in Dijon is in red, the reception site in Revest du Bion in blue and Lausanne is in green. The red half circle is the direction of the sent signal [7]. 4
2 Emission site for the GRAVES system. There are 4 panels containing 28 patch antennas each. 5
3 Schemes of the device at the emission. (a) profile view (b) front view. The azimuth opening is $8°$, the elevation opening is $20°$ and the pitch angle is $60°$. 5
4 Reception site for the GRAVES system. There are 100 antennas dispatch in a circle area. 5
5 Scheme of the bistatic system. Tx is the transmitter, Rx is the receiver, β is the angle formed by the Tx, the object and the Rx, v is the speed of the object, δ is the angle between the direction of the object and the bisector of β and w is the projected speed. 5
6 Variation of $\vec{w}$ with the frequency shift Δf for different β. β is plotted from $0°$ to $140°$ by steps of $10°$. 6
7 (a) Representation of the ellipsis on the globe. The object is on the blue curve. (b) Ellipsis used for the estimation of possible β. a is the long radius, b is the short radius and x is the long radius minus half the distance between Lausanne and Dijon. 6
8 Number of occurrences for different angles and for 3 values of a and for a constant b of $400\,\mathrm{km}$. $a = 500\,\mathrm{km}$ (blue), $a = 1000\,\mathrm{km}$ (purple) and $a = 1500\,\mathrm{km}$ (green). 7
9 Number of occurrences for different angles and for 3 values of b and for a constant a of $1000\,\mathrm{km}$. $b = 400\,\mathrm{km}$ (blue), $b = 700\,\mathrm{km}$ (purple) and $b = 1000\,\mathrm{km}$ (green). 7
10 Yagi's antenna for VHF $(140 - 160\ MHz)$ 7
11 ADC (Analog digital converter) Dongle Funcube Pro+ 8
12 Example of possible output of the program Spectrum Lab V2. The frequency variation is along the $x - axis$ and the time along the $y - axis$. [15] 8
13 Scheme of the propagation path. R is the distance between the object detected and the transmitter/receiver device. 8
14 Evolution of the frequency with time. f_0 is the lowest value of frequency possible, T is the period of one ramp and B is the bandwidth. 9
15 Sent (blue) and received (red) signals. f_S is the shift in frequency due to Doppler's effect, τ is the time for the signal to reach the object and come back to the receiver, t_l is the total time of completed ramps, t_s is the time of the current ramp and m is the index of the ramp with M the total number of ramps. 10

16 Blocks representation of FMCW containing : modulator, VCO (voltage controlled oscillator), power and voltage amplifiers, splitter, mixer, antennas and computer. Blue part is the emitter and green part is the receiver. 11
17 Output of the simulation after 2D Fast Fourier Transform (FFT). There are 3 couples of 2 points. 11
18 Output of the simulation after 2D FFT with circles marking the redundancy in blue red and green. 11
19 Results obtained by the university of Hamburg explaining the redundancy obtained. 12
20 Scheme of passive detection. R_{x1} and R_{x2} are two receiver sites. 12
21 Triangulation for passive detection with three receivers (R_{x1}, R_{x2} and R_{x3}). The green arrows are the path of the reflected wave. 12
22 $s_{r1}(t)$ in orange, $s_{r2}(t+\tau)$ in green and the cross correlation $R(\tau)$ in blue (for a $t = 0$ and a $\tau = 8$). 13
23 Situation for the computation of the angle. R_{x1} and R_{x2} are two receivers, d is the distance between the two sites, d_{add} is the additional distance travelled by the wave, τ is the additional time to travel d_{add} and θ is the angle of the incoming wave. 13
24 Situation for the tracking of an object based on cross correlation at different times. R_{x1} and R_{x2} are two receiving sites and d is the distance between them. 14
25 Situation for the computation of the angular resolution 14

List of Tables

I Simulation parameters (speed and range) of 3 objects 11

***Abstract*—This report is a study of different systems to detect space objects using radio frequencies. Three systems are studied to determine the best option: bistatic radar, Frequency Modulated Continuous Waves (FMCW) and passive detection. The purpose of the detection is to gain information on the location, speed and range of the object through signal and data processing.**

I. Introduction

Nowadays, engineers are interested in creating a catalogue of all the space objects in orbit around the Earth. The purposes of creating such a catalogue are predicting trajectory in order to avoid a collision with a spaceship, space cleaning and many others. This can be done with an optical telescope or with a radio frequency (RF) system [1]. The main advantage of a radio frequency system over an optical system is the transmission when the sky is cloudy. For an object to be detected by an optical system, it also needs to be geostationary.

Different methods are used in order to detect space debris, meteors, satellites or anything else in orbit. Bistatic radar is a first approach and is widely used by countries to catalogue the objects over their territory. Examples of such a technology are the telescope GRAVES in France or BRAMS in Belgium [2], [3]. Another approach is passive detection. This method is interesting because the objects are detected by re-using RF emitters already implemented for other purposes. It uses triangulation techniques like the Global Positioning System (GPS). A last system known as FMCW will be explained. The primary application of this system is short range detection but it can be extended to the distances of objects in orbit.

This report will detail these three methods with a mathematical approach to explain the physics behind each system. Afterwards, the signal and data processing will be described to understand the working principles of the different blocks. Chapter VI will recommend the best solution according to the writer and then a brief conclusion will sum up the main points.

II. GRAVES

A. Overview

1) Situation: GRAVES is the acronym for Grand Réseau Adapté à VEille Spatiale and is a French military radar developed by the French aerospace research establishment (ONERA) [4]. The purpose of this satellite is to fill a catalogue regrouping the space debris but also satellites and meteors. The range of this radar is between $400\,\mathrm{km}$ and $1000\,\mathrm{km}$. The carrier frequency used ($143.05\,\mathrm{MHz}$) is in the VHF band ($30\,\mathrm{MHz}$ - $300\,\mathrm{MHz}$) [5] and the emission is done with Continuous Waves (CW) [4]. The radar is called bistatic meaning that the emission and reception sites are not at the same place. The emission is located near Dijon in Broyes les Pesnes (47,3477 N – 5,5136 E) and the reception is in the South of France (Revest du Bion : 44,0706 N – 5,5347 E) [6].

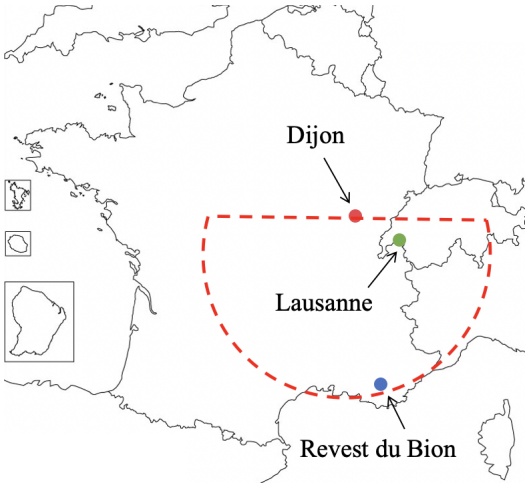

Fig. 1. Map of the situation of GRAVES in France. The emission site in Dijon is in red, the reception site in Revest du Bion in blue and Lausanne is in green. The red half circle is the direction of the sent signal [7].

2) Principle: The emission site is composed of four panels made of 28 patch antennas each as represented on Figure 2. These panels are pointing southwards and are creating an opening of $180°$ [6]. In fact, the whole $180°$ opening in not scanned at the same time because it is not possible to both have high directivity and large opening. Therefore, these antennas are scanning antennas which means that the direction of the main lobe is moving in time. Each panel is responsible for $45°$ of the opening and the main lobe is $8°$ wide in azimuth direction. The elevation opening is $20°$, the tilt of the panels is $60°$ and the period of scanning is $20\ s$ meaning that the lobe moves at a speed of $2.25°/s$.

Fig. 2. Emission site for the GRAVES system. There are 4 panels containing 28 patch antennas each.

The global situation is represented on Figure 3 and this type of emission technique allows the constant illumination of 4 regions of the sky [6], [8].

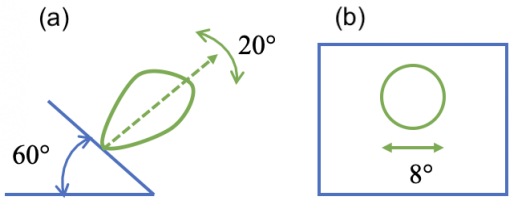

Fig. 3. Schemes of the device at the emission. (a) profile view (b) front view. The azimuth opening is 8°, the elevation opening is 20° and the pitch angle is 60°.

The reception of the information is done using a set of antennas as shown in Figure 4. For the GRAVES system, there are exactly 100 antennas dispatched on a circle. This array of antennas catches a signal coming from a certain direction and each antenna converts the received wave in a digital signal to process it with a computer. Based on the 100 signals, it is possible, using phase delays, to construct a very narrow lobe giving the direction of the incoming electromagnetic wave [6].

The signal detected will have a frequency shift compared to the carrier frequency because of the Doppler effect. Using this difference, a notion of speed can be found but it won't be the exact speed of the object. The value found will be the projection of the speed in the direction of the bisector of the angle formed between the transmitter, the object and the receiver. This will be detailed later. GRAVES emission waves are also used for the FRIPON network [9]. This cooperation is a French initiative using the bistatic principle with receptors dispatched every $50 - 100\ km$ in France allowing to cover the whole French sky. The positioning of all the reception sites can be found on the internet [9]. One of the main military advantages of GRAVES is the detection of spy satellites.

Fig. 4. Reception site for the GRAVES system. There are 100 antennas dispatch in a circle area.

B. Mathematical approach

As explained in section II-A2, the GRAVES system is able to provide information on the speed and position of the spatial object.

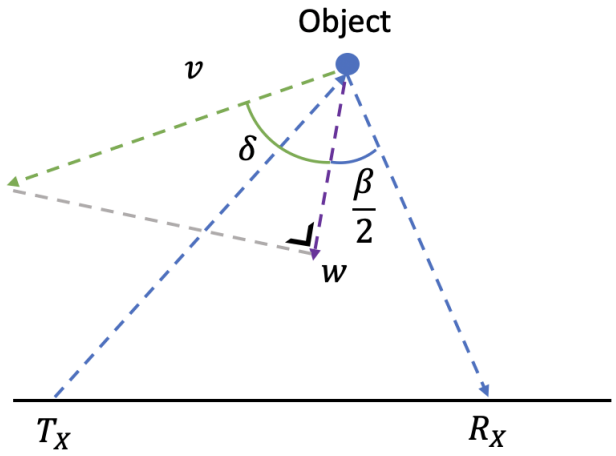

Fig. 5. Scheme of the bistatic system. Tx is the transmitter, Rx is the receiver, β is the angle formed by the Tx, the object and the Rx, v is the speed of the object, δ is the angle between the direction of the object and the bisector of β and w is the projected speed.

The speed of the object is found based on the Fizeau-Doppler effect. Once the emitted wave

encounter an object, it will be reflected towards the Earth with a new frequency. The situation is represented on Figure 5 where δ is the angle of the projection, β is the bistatic angle (angle between the emitted and received waves), $\vec{v}$ is the speed of the object and $\vec{w}$ is a projection of this speed onto the bisector of angle β.

Tx and Rx will be used to describe the emitter and receiver. The frequencies linked to those sites are respectively f_{Tx} and f_{Rx}. The variation of frequency Δf is then defined as:

$$\Delta f = f_{Rx} - f_{Tx} \tag{1}$$

It is possible to link this difference in frequency to the speed of the object using equation (2). It is the definition of the Doppler effect.

$$\Delta f = \frac{2 f_{Tx} \cos\left(\frac{\beta}{2}\right)}{c} \cos(\delta) ||\vec{v}|| \tag{2}$$

Where c is the speed of light, f_{Tx} the carrier frequency of the emitter, β the bistatic angle and $\vec{w}$ the projection of the speed. By looking back at the definition of $\vec{w}$ on Figure 5, the expression of equation (2) can be simplified using the following property.

$$||\vec{w}|| = ||\vec{v}|| \cos(\delta) \tag{3}$$

Combining equations (2) and (3), gives equation (4).

$$\Delta f = \frac{2 f_{Tx} \cos\left(\frac{\beta}{2}\right)}{c} ||\vec{w}|| \tag{4}$$

Before detailing further, two statements can be made. Multiple observation sites can be implemented based on the reflected wave but the bistatic angle β is unknown and can't be computed using different antennas. Indeed, if the reception site changes, then the R_x on Figure 5 would change and so would β. A second observation is the particular case where $\delta = 90°$. In that situation, the projection of $\vec{v}$ onto the bisector of the β angle axis would be null.

The problem is that there is one equation for two unknowns (β and $\vec{w}$). Therefore, a chart is made where w is plotted as a function of Δf for different values of β (see Figure 6).

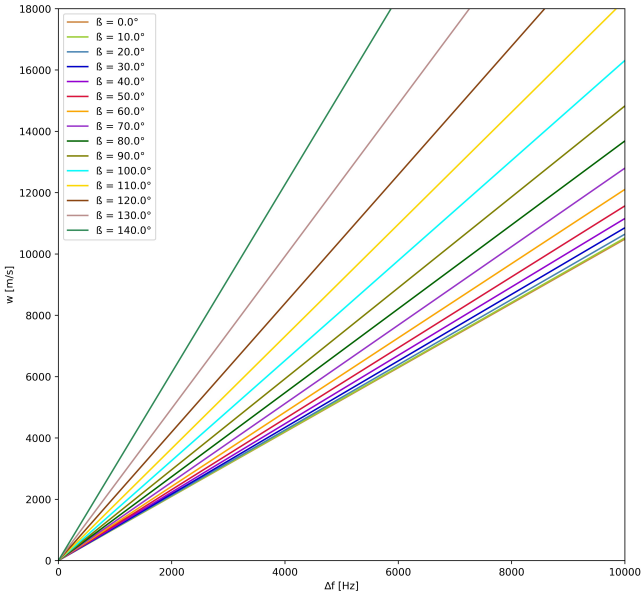

Fig. 6. Variation of $\vec{w}$ with the frequency shift Δf for different β. β is plotted from $0°$ to $140°$ by steps of $10°$.

Figure 6 shows that for small angles, the variation of speed for a same frequency shift is small. This variation increases a lot when the bistatic angle increase. This might be a problem so an analysis of the possible angles is done. Indeed, for example an angle of $140°$ is very unlikely to occur in the kind of detection performed in this project.

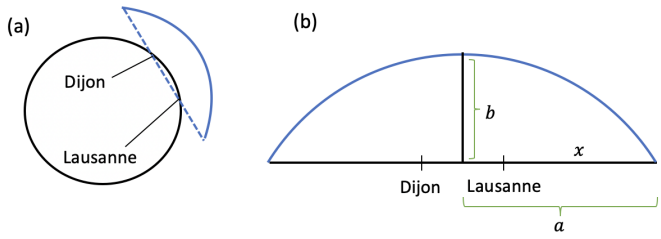

Fig. 7. (a) Representation of the ellipsis on the globe. The object is on the blue curve. (b) Ellipsis used for the estimation of possible β. a is the long radius, b is the short radius and x is the long radius minus half the distance between Lausanne and Dijon.

To see the range of interesting angles for the project scope, a simulation is performed. As a reminder, here is the equation of an ellipsis:

$$\frac{x^2}{a^2} + \frac{y^2}{b^2} = 1 \tag{5}$$

Where a and b are the long and short radius of the ellipsis as shown on Figure 7.

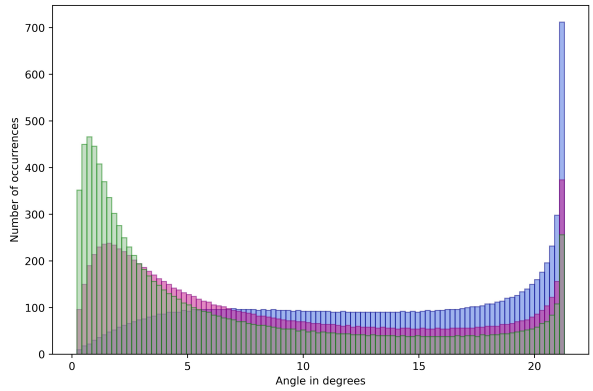

Fig. 8. Number of occurrences for different angles and for 3 values of a and for a constant b of $400\,\mathrm{km}$. $a = 500\,\mathrm{km}$ (blue), $a = 1000\,\mathrm{km}$ (purple) and $a = 1500\,\mathrm{km}$ (green).

The distance between Dijon and Lausanne is $150.37\,\mathrm{km}$ [10]. Figure 8 shows three probability density function (*PDF*) for a constant value of $b = 400\,\mathrm{km}$ and different values of x : $500\,\mathrm{km}$ (blue), $1000\,\mathrm{km}$ (purple) and $1500\,\mathrm{km}$ (green). Note that b is set to the smallest value of the detection range as it will create the highest angles. The more the value of a $(= x + \frac{d_{D-L}}{2})$ increases, the highest is the probability to have a small angle as shown on Figure 8 (where d_{D-L} = distance between Dijon and Lausanne).

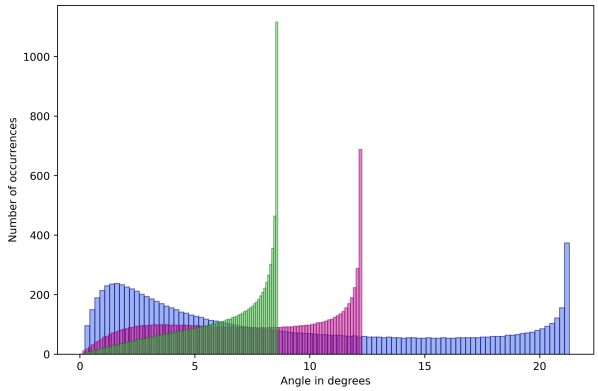

Fig. 9. Number of occurrences for different angles and for 3 values of b and for a constant a of $1000\,\mathrm{km}$. $b = 400\,\mathrm{km}$ (blue), $b = 700\,\mathrm{km}$ (purple) and $b = 1000\,\mathrm{km}$ (green).

The same analysis can be done but this time by changing the value of b. The project is focusing on detection between $400\,\mathrm{km}$ and $1000\,\mathrm{km}$ so Figure 9 shows the results for three ellipsis with b set to $400\,\mathrm{km}$ (blue), $700\,\mathrm{km}$ (purple) and $1000\,\mathrm{km}$ (green) and a is constant. When the object is higher in the sky, the PDF shows a higher probability of obtaining smaller angles.

The conclusion of this small study on the possible β angles shows that the values stay relatively small (between $0°$ and $20°$). Looking back at Figure 6, the curves with $\beta = 0°, 10°$ and $20°$ are almost similar meaning that β won't impact much the result.

C. Block system

1) Antenna: The first element of the chain is the antenna. The system here is developed for one antenna but can be replicated to detect the angular position of the space object. Because the carrier frequency is $143.05\,\mathrm{MHz}$, an antenna with a range around this value is needed. The literature references the Yagi antenna as having a reception band of $140\,\mathrm{MHz}$ - $160\,\mathrm{MHz}$ [11].

Fig. 10. Yagi's antenna for VHF $(140 - 160\ MHz)$

2) Preamplifier: The received signal converted in voltage by the antenna has small values and needs to be amplified in order to attain the digital processing part (computer). To do so, a preamplifier is placed at the beginning of the transmission line. This strategic positioning allows to amplify the signal before adding noise due to the imperfection of the transmission line.

3) Transmission line: As explained in the above paragraph, a transmission line is used to connect the antenna and the computer. Indeed, the antenna will most probably be outside on a roof but the processing part could be done inside and therefore a cable is needed. An usual method of transmission is the coaxial cable.

4) Band pass filter: A band pass filter would be placed at the end of the transmission line to filter the noise and the perturbation due to the transmission line. The band pass filter is usually created with a RLC circuit.

5) Receiver: Now that the signal has reached the processing site at the processing site, it needs to be converted from the analog to the digital system. Indeed, it is easier to perform data processing than signal processing. The block for this conversion is an Analog Digital Converter (ADC).

Fig. 11. ADC (Analog digital converter) Dongle Funcube Pro+

The ADC presented in Figure 11 is a Dongle Funcube Pro+ [12] and could be used because it has a USB port at one end and a wire connection at the other (SMA connection) [13]. This device needs to be calibrated on the carrier frequency using the program contained in the package (Dongle Pro+ Control V2).

6) Program: Spectrum Lab V2 is an open source program which provides waterfall plots of the frequency with respect to the time. Based on the time of detection and the value of the Doppler shift, the type of objects can be found. For example, a huge speed detected in a small amount of time can be associated to a meteor. Figure 12 is an example of the output of the program for a meteor [14].

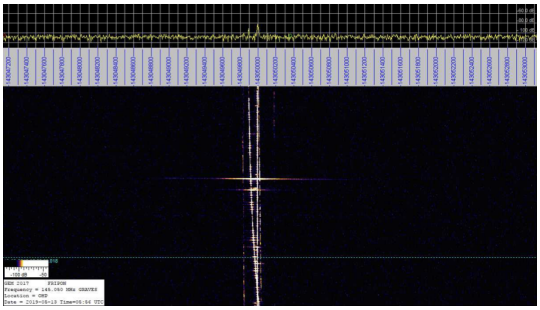

Fig. 12. Example of possible output of the program Spectrum Lab V2. The frequency variation is along the $x-axis$ and the time along the $y-axis$. [15]

III. FMCW

A. Overview

FMCW stands for frequency modulated continuous waves and is another way to detect objects. The advantage of this technique is that the emitting and receiving sites are at the same place allowing to correlate the signals very easily. FMCW detection is performed with a beat signal $s_b(t)$ being the correlation between the sent signal and the received signal. This beat signal is sampled and then transformed (using Fourier 2D) in the frequency domain. This allows to obtain information on both the speed and range of an object after linear transformation of the axis. This methodology will be further developed in section III-B [16].

The main difficulty with this kind of device is the interference due to mitigation with other signals in the same band. This interference causes the apparition of ghost targets in the frequency domain [17].

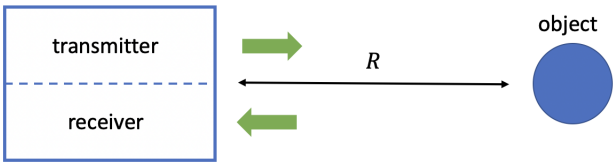

Fig. 13. Scheme of the propagation path. R is the distance between the object detected and the transmitter/receiver device.

The situation of the FMCW system is shown in Figure 13. Where R is the range of the object.

B. Mathematical approach

The following mathematical development comes from a document published by the HAL open sciences [18]. To begin with, the variation of the frequency as a function of the time is defined according to equation (6). This equation represents the evolution shown on Figure 14.

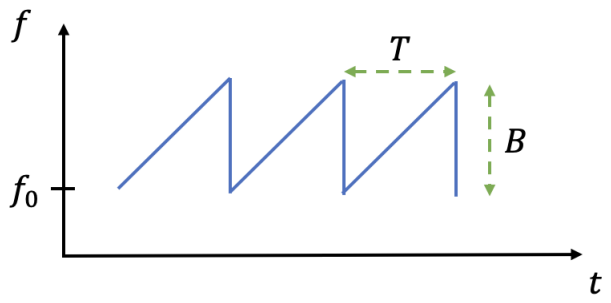

Fig. 14. Evolution of the frequency with time. f_0 is the lowest value of frequency possible, T is the period of one ramp and B is the bandwidth.

Where f_0 is the minimum frequency, B the bandwidth and T the period.

$$f(t) = f_0 + \frac{B}{T}t \quad t \in [0; T] \tag{6}$$

Based on this frequency, the emitted signal ($s_e(t)$) can be defined as the amplitude (A_e) multiplied by the exponential of the phase (ϕ) times the complex number j.

$$s_e(t) = A_e e^{j\phi} \tag{7}$$

The phase is simply the integral of the frequency between 0 and t multiplied by 2π [19].

$$\phi = 2\pi \int_0^t f(t')\,\mathrm{d}t' = 2\pi(f_0 t + \frac{B}{2T}t^2) \tag{8}$$

By combining the two previous equations, the expression of the signal transmitted (s_e) is found and written :

$$s_e(t) = A_e e^{j2\pi(f_0 t + \frac{B}{2T}t^2)} \tag{9}$$

The effects of the propagation will now be considered and the reflected/received signals will be obtained. To do so let's refer to the situation illustrated in Figure 13 where R is the distance between the device and the detected object. The time taken to propagate the distance R is simply $\frac{R}{c}$ and will be written as $\frac{\tau}{2}$. Therefore, just after reflection, the expression is:

$$s_{refl}(t) = K A_e e^{j2\pi(f_0(t-\frac{\tau}{2}) + \frac{B}{2T}(t-\frac{\tau}{2})^2 - f_S t)} \tag{10}$$

Where K is an attenuation coefficient and f_S the shift in frequency (see Figure 15). Then, the wave propagates back to the emission/reception site and thus travels the distance R once again. This implies a new delay of $\frac{\tau}{2}$ and equation (10) becomes:

$$s_r(t) = K' A_e e^{j2\pi(f_0(t-\tau) + \frac{B}{2T}(t-\tau)^2 - f_S(t-\frac{\tau}{2}))} \tag{11}$$

Where K' is the update attenuation factor K due to the propagation path. The last step is to mix together the sent signal and the complex conjugate of the received signal to obtain $s_b(t)$, the beat signal.

$$\begin{aligned} s_b(t) =& s_e(t) s_r^*(t) \\ =& K' A_e^2 e^{j2\pi(f_0 t + \frac{B}{2T}t^2 - f_0(t-\tau) - \frac{B}{2T}(t-\tau)^2 + f_S(t-\frac{\tau}{2}))} \\ =& K'' e^{j2\pi(\phi_0 - \frac{B}{T}t\tau + f_S t)} \end{aligned} \tag{12}$$

In the above expression, all the terms dependent on t remain untouched and the others are regrouped in a new term (ϕ_0). K'' is an attenuation factor depending on the path of propagation and ϕ_0 is:

$$\phi_0 = f_0\tau - \frac{B}{2T}\tau - f_S\frac{\tau}{2} \tag{13}$$

The beat frequency (f_b) is the interesting part to extract from the beat signal and is in the exponential. Knowing that the beat signal can be expressed as the exponential of a function with this form $ft + \phi$ and having identify the independent term $\phi = \phi_0$ (13), the beat frequency is :

$$f_b = \frac{B}{T}\tau + f_S = \frac{2BR}{cT} + f_S \tag{14}$$

The beat frequency is expressed in function of the two unknowns of the problem : the speed and the distance of the object (the speed is embedded in f_S). The beat signal can be rewritten :

$$s_b(t) = K'' e^{j2\pi(\phi_0 + f_b t)} \tag{15}$$

To obtain a plot of the frequency shift and the distance, it is needed to decompose t into t_s (short time) and t_l (long time).

1) t_s : time on one ramp ($0 < t_s < T$)
2) t_l : define the current ramp ($= mT$) with $m = 0, 1, 2, ..., M-1$ (M is the total number of ramps). It can be interpreted as the number of "complete" ramps.
3) $t = t_s + t_l$: is the current time

For example if the current time is the middle of the fourth ramp, $t_s = \frac{T}{2}$, $t_l = 4T$ and $t = 4.5T$. By substituting the expression of t in equation (15), equation (16) is obtained.

$$s_b(t_s, t_l) = K'' e^{j2\pi\phi_0} e^{j2\pi f_b t_s} e^{j2\pi f_S t_l} \quad (16)$$

This expression depends on t_s and t_l but by performing a 2D Fourier transform, the resulting expression will depend on f_b and f_S. First, a sampling has to be performed on both variables. For the long time, it has already be implicitly done because it is the number of ramps $t_l = mT$. For the short time, a sampling period T_s is taken in order to have N samples. This period is defined as $\frac{T}{N}$ and therefore, $t_c = nT_s$ with $n = 0, 1, 2, ..., N-1$. The sampled signal is equation (17).

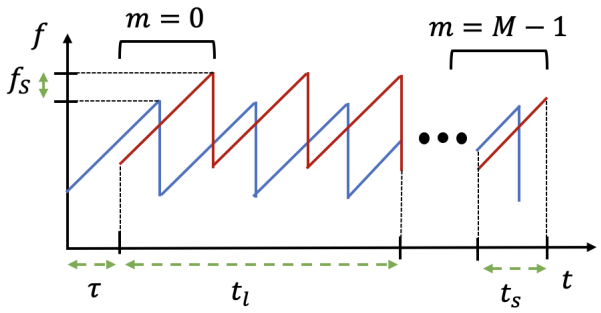

Fig. 15. Sent (blue) and received (red) signals. f_S is the shift in frequency due to Doppler's effect, τ is the time for the signal to reach the object and come back to the receiver, t_l is the total time of completed ramps, t_s is the time of the current ramp and m is the index of the ramp with M the total number of ramps.

Figure 15 shows the sent and received signals for different ramps. Based on the explanation here above, to obtain information on the frequency shift, it is needed to have a study of multiple ramps.

$$s_b(t_s, t_l) = K'' e^{j2\pi\phi_0} e^{j2\pi f_b n T_s} e^{j2\pi f_S m T} \quad (17)$$

τ_{max} is the maximal delay corresponding to the maximal path. After performing the 2D Fourier transform, the continuous signal (S_b^c) looks like equation (18).

$$S_b^c(f, f') = KA_e e^{j2\pi\phi_0}(T-\tau_{max}) e^{-j\pi(f-f_b)(T+\tau_{max})} sinc(\pi(f-f_b)(T-\tau_{max})) \times (M-1)T e^{-j\pi(f'-f_S)(M-1)T} sinc(\pi(f'-f_S)(M-1)T) \quad (18)$$

C. Block system

The structure of the circuit presented in this section comes from the work done by a Turkish university [20]. The full chain is presented on Figure 16 and is made of a modulator, a VCO (voltage controlled oscillator), power and voltage amplifiers, a splitter, a mixer and the antennas. The blue and green parts are respectively the emitter and the receiver.

1) Modulator: The purpose of the modulator block is to create a triangular and a square signal. The triangular signal is the one sent and the square signal is used for synchronization. For the moment, the signal is varying in voltage but to perform FMCW, a variation in frequency is needed. This is where the VCO comes in play.

2) Voltage Controlled Oscillator (VCO): Based on the voltage signal, the VCO produces the desired frequency signal. The center frequency and the band can be chosen depending on the design of the VCO. The output signal is passed in a power amplifier before arriving at the splitter.

3) Splitter: The splitter is used to divide the signal between two branches. The first one will directly be emitted by the antenna (T_X) and the second one will go into the mixer. Because of this separation, the power of the signal is divided by 2 (equivalent to $-3dB$). The emitted and received signals need to be mixed in a mixer as explained previously in section III-B.

4) Mixer: The inputs of the mixer are the emitted signal and the received signal amplified in power. Indeed, the signal received at the R_X antenna is usually low in power. The output of the mixer block is the beat signal $s_B(t)$ as defined in section III-B. This signal is then

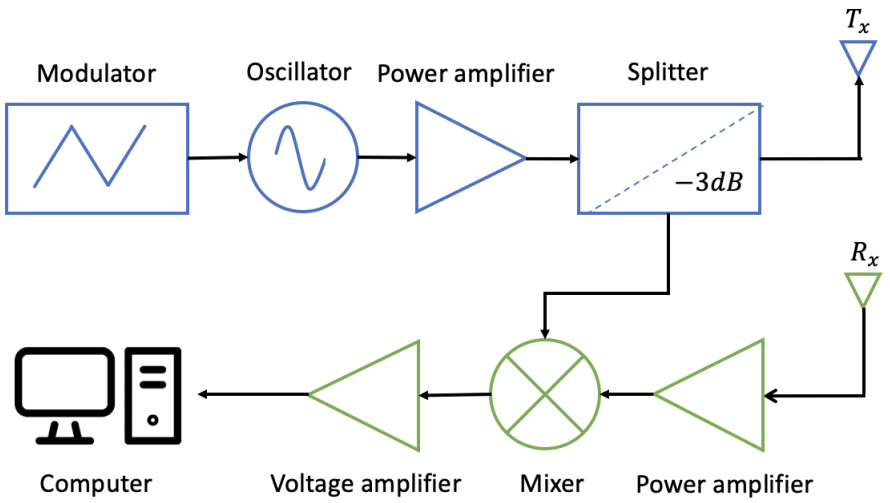

Fig. 16. Blocks representation of FMCW containing : modulator, VCO (voltage controlled oscillator), power and voltage amplifiers, splitter, mixer, antennas and computer. Blue part is the emitter and green part is the receiver.

amplified in voltage before arriving in the computer.

5) Computer: There is a conversion from analog to digital like in the GRAVES system and then the data is processed. No real data are acquired because this is a research work but a simulation of 3 objects is done in Python. The speeds and ranges of the 3 objects are described in Table I. The values taken are typical plausible values that the FMCW radar will detect once implemented.

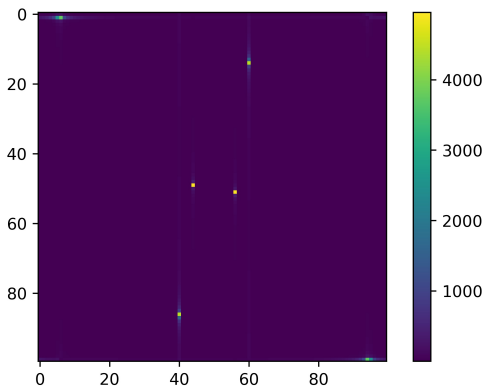

Fig. 17. Output of the simulation after 2D Fast Fourier Transform (FFT). There are 3 couples of 2 points.

the output after performing the fast Fourier transform in 2 dimensions is shown in Figure 17. This Fourier transform is performed on a $M \times N$ matrix with in this case $M = N = 100$. This explains the value of the axis on Figure 17. The higher the value of M and N the more precise the FFT will be (less pixelized).

TABLE I
SIMULATION PARAMETERS (SPEED AND RANGE) OF 3 OBJECTS

Parameter	Object 1	Object 2	Object 3	Units
Speed	200	2000	20000	m/s
Range	100	50	800	km

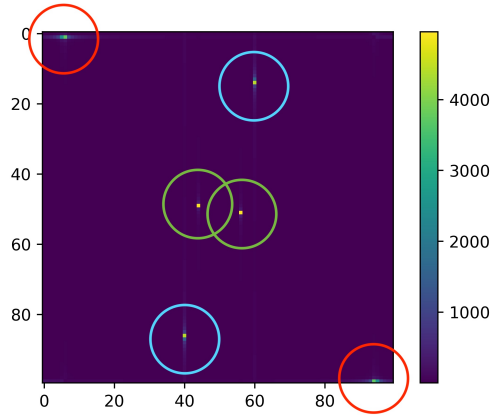

Fig. 18. Output of the simulation after 2D FFT with circles marking the redundancy in blue red and green.

The first observation is the appearance of 6 points instead of 3. In fact, there is a redundancy in the

output as shown on Figure 18.

The work done on FMCW by the university of Hamburg explains the appearance of twice the number of objects. By looking at the $x-axis$ of Figure 19, there is a repetition of the same information. Indeed, the 2 yellow lines have the same x value (distance of $4.8\,\mathrm{km}$) but are represented twice. Note that the velocity has the same value with opposite signs.

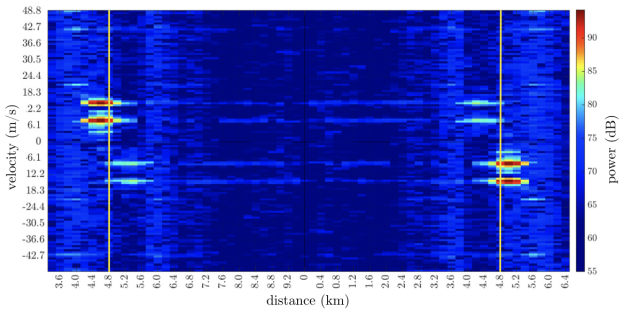

Fig. 19. Results obtained by the university of Hamburg explaining the redundancy obtained.

The computer processing is not part of the scope of this project so it will not be further developed. For more information refer to [17].

IV. Passive detection

A. Overview

Passive detection is a low cost solution to detect space objects as only the receivers have to be implemented. The emitters are unknown sources of RF signals used to measure the reflections on objects. This phenomena is therefore dependent on the nature of the environment. The situation is represented on Figure 20. The main disadvantage of this type of detection is that the sent signal is unknown. For satellites, the allocated frequencies are in the ISM band ($2.4\,\mathrm{GHz}$ - $2.483\,\mathrm{GHz}$) [21], [22] which is narrow enough to consider a fixed value for the sent frequency. The objective now is to recover the frequency after the reflection on the space object in order to obtain the Doppler shift. To do so, Costas loops [23] are implemented to elevate the received signal to the N^{th} power and retrieve the frequency. This will be further developed in the mathematical approach (see section IV-B).

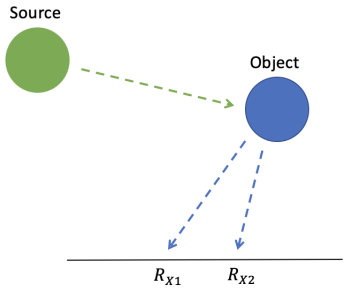

Fig. 20. Scheme of passive detection. R_{x1} and R_{x2} are two receiver sites.

The speed of the object is found via the Doppler shift but the position is still unknown. The position of the object in the sky is obtained using time delay between different antennas. At least three antennas are needed to obtain both the elevation and azimuth angles. The time delay is found by doing a cross correlation between the two received signals. Knowing the time delay, the additional distance traveled between the two receiving sites can be calculated. Based on this distance and the separation between the two sites, it is possible to compute the angle. If only two antennas were used, the elevation angle would be found but not the azimuth angle as shown on Figure 21. This principle is called triangulation and is used for example in GPS technology. This part will also be approached using mathematical background in section IV-B.

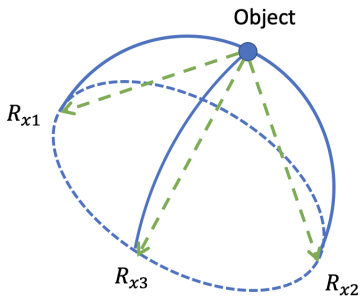

Fig. 21. Triangulation for passive detection with three receivers (R_{x1}, R_{x2} and R_{x3}). The green arrows are the path of the reflected wave.

B. Mathematical approach

The two main objectives of this section are to obtain the frequency after reflection on the object and the time delay even though the sent signal is unknown. The following development is based on the work done by the Canadian defense [24].

The problem with the frequency is that most of the satellites use a PSK (Phase Shift Keying) modulation which suppresses the carrier frequency. However, as explained in section IV-A, the carrier frequency is in a very narrow band and will be considered constant ($f_c = 2.4\,\mathrm{GHz}$). A PSK signal can be written according to equation (19) where f_D is the frequency after reflection, $n = 0, 1, ..., N-1$ is the index of modulation and N is the order of modulation.

$$s_n(t) = e^{j2\pi(f_D t + \frac{n}{N})} \tag{19}$$

For example, in a BPSK ($N = 2$), the two signals would be $s_0(t) = e^{j2\pi f_D t}$ and $s_1(t) = e^{j2\pi f_D t + \pi}$. Based on $s(t)$, the signal obtained at the base stations follows equation (20).

$$s_r(t) \approx (1 - \frac{\dot{R}}{c})\ e^{j2\pi((1-\frac{\dot{R}}{c})f_D(t-\frac{R}{c})+\frac{n}{N})} \tag{20}$$

By raising the expression to the N^{th} power, the term with the n in the exponential disappears (always a multiple of 2π). Therefore, the main component is the frequency after reflection (f_D) multiplied by a known factor N as shown in equation (21).

$$\begin{aligned} s_r^N(t) &\approx (1 - \frac{\dot{R}}{c})^N\ e^{j2\pi(N(1-\frac{\dot{R}}{c})f_D(t-\frac{R}{c})+n)} \\ &= (1 - \frac{\dot{R}}{c})^N\ e^{j2\pi N((1-\frac{\dot{R}}{c})f_D(t-\frac{R}{c}))} \end{aligned} \tag{21}$$

For the time delay, the principle is the cross correlation between the two received signals. if $s_{r1}(t)$ and $s_{r2}(t+\tau)$ are received, where τ is the time delay as shown on Figure 23, then the expression of the cross correlation is found via equation (22).

$$R(\tau) = \int_{-\infty}^{\infty} s_{r1}^*(t) s_{r2}(t+\tau)\,\mathrm{d}t \tag{22}$$

The cross correlation will be maximal at the time of the delay. For example, by simulating two gaussian curves centered in $x = 0$ and $x = 8$, the cross correlation is maximal in $x = 8$, the value of the time delay. The simulation is plotted in Figure 22.

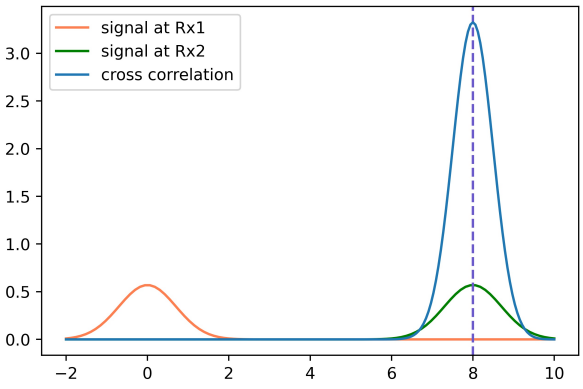

Fig. 22. $s_{r1}(t)$ in orange, $s_{r2}(t+\tau)$ in green and the cross correlation $R(\tau)$ in blue (for a $t = 0$ and a $\tau = 8$).

Based on the knowledge of τ and for a wave travelling at the speed of light ($c = 299\,792\,458\,\mathrm{m/s}$) the additional distance of propagation is found with equation (23).

$$d_{add} = c\tau \tag{23}$$

Knowing the distance between the two antennas (d) and the distance d_{add}, it is possible to find the angle θ on Figure 23.

$$\cos(\theta) = \frac{d_{add}}{d} \iff \theta = \arccos(\frac{d_{add}}{d}) \tag{24}$$

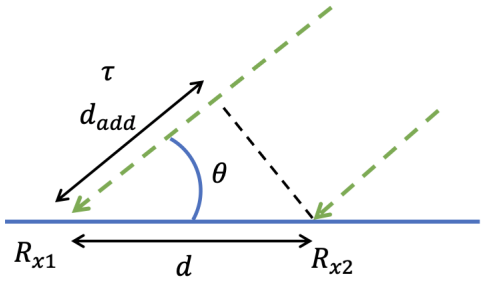

Fig. 23. Situation for the computation of the angle. R_{x1} and R_{x2} are two receivers, d is the distance between the two sites, d_{add} is the additional distance travelled by the wave, τ is the additional time to travel d_{add} and θ is the angle of the incoming wave.

Applying the same methodology between antennas R_{x2} and R_{x3} would give another angle in another plane and therefore another information on the position in the sky. If the third antenna is aligned with the first and second then the azimuth

information can't be recovered.

The method just explained can be used to track an object in the sky if data has been recorded for a long enough period (eg : a day). In this case, by changing the value of τ in the cross correlation computation, it is possible to aim to different directions in the sky as shown on Figure 24. When the value of the cross correlation is high for a given t_0, it means that the object was found. Then for time $t_1 = t_0 + \Delta t$, the cross correlation will be high for another value of τ and therefore a new position in the sky is found. Note that because the distance d is smaller than the distance between the antennas and the object, a paraxial approximation is done to still have a situation as in Figure 23.

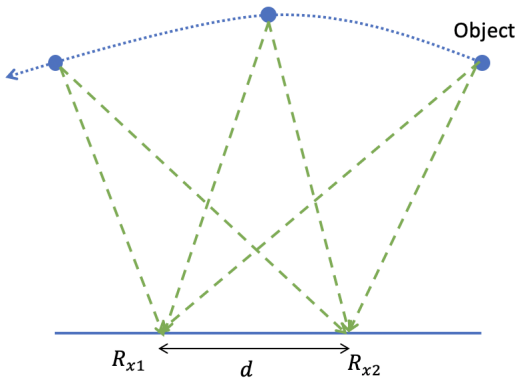

Fig. 24. Situation for the tracking of an object based on cross correlation at different times. R_{x1} and R_{x2} are two receiving sites and d is the distance between them.

Another way to obtain the angle θ in Figure 23 is by isolating the phase difference. If the signals received at R_{x1} and R_{x2} are mixed, two terms will appear : one oscillating at twice the frequency and the other one only containing the phase. By low pass filtering, the phase can be obtained:

$$\phi = 2\pi \frac{d}{\lambda} \sin(\theta) \tag{25}$$

The finding of angles is explained for passive detection but can be extended to every system having multiples reception sites like the GRAVES system. Indeed, it was here developed for one antenna but can be done using multiples antennas. Whenever there is more than one antenna, the notion of angular resolution appears. This will be detailed in section V

C. Block system

The block design for passive detection is essentially the same as the GRAVES system. There is an antenna, a preamplifier and a coaxial cable. Then an ADC makes the conversion to the digital world and computation can be done. This time, all the signals coming from the different antennas must be analysed together. Once all the signals are at the computer, the angles can be computed.

V. Angular resolution

The angular resolution is a measurement describing the precision of the detection. If two space objects are really close when they are detected, they could be mixed up and the information received would be irrelevant as it could come from either objects. The angular resolution is defined in equation (26) where S_A is the distance between the two space objects, R is the range and α is the angle between the maximal power and half power ($-3\,\mathrm{dB}$) [25], [26], [27].

$$S_A \geq 2R \sin\left(\frac{\alpha}{2}\right) \tag{26}$$

Figure 25 shows the situation. By simple trigonometry, equation (26) is easily demonstrated.

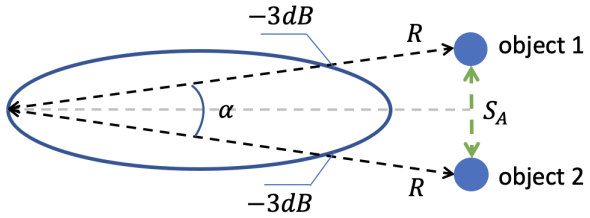

Fig. 25. Situation for the computation of the angular resolution

The resolution angle (α) can also be defined with respect to the array. It depends on the wavelength (λ) and the distance between the two most distant antennas (D). Indeed, the formula is computed for each possible couple of antenna and the most restrictive pair is kept. D is called the baseline.

$$\alpha = \frac{\lambda}{D} \tag{27}$$

VI. Recommendation

The study done for the moment shows 3 types of detection each presenting pros and cons. This section presents my opinion on the system to implement.

If data has to be acquired rapidly, I would recommend to implement the GRAVES system. Indeed, the emitter is already built and the receiver is easy to create. It has been done by radio amateurs in Europe and should not be too difficult. The major inconvenience is that only the speed in the direction of the bisector of the β angle is known. There is no notion of range nor direction with only one antenna. This would thus just inform on the presence of the object and have some notion of speed ($\vec{w}$).

In passive detection, like the GRAVES system, the emission is already present and only the reception needs to be implemented. At least three antennas are needed on three different sites to locate objects. This gives no information on the range.

In my opinion, the best system is the detector using FMCW. This system is completely adaptable to our needs where GRAVES is imposed by the french army. Indeed, based on the target range, the resolution and other factors, the parameters can be adapted. FMCW both gives information on the speed and the range of the object using Fourier's transform. The report of the HAL even shows that there are techniques to retrieve information on the angles and therefore have an exact location in the sky. The disadvantage of this system is that it is more complex to design and implement.

A possible idea could be to combine different systems. For example, the FMCW system would be used for the speed and range and the passive detection or the GRAVES system with multiple antennas for detecting the position in the sky. A work of identification would have to be conducted to link the information detected on both system to the objects.

VII. Conclusion

This work was done for the Space Situational Awareness (SSA) Team in order to develop a radio frequency telescope.

Three ways to detect objects orbiting around the Earth were investigated and each of them presents pros and cons. The systems developed are GRAVES, FMCW and passive detection. The purpose of the future system is the detection of position, range and speed of the objects. The mathematical background as well as the black boxes are presented to implement the project.

To go further, the system could be upgraded in order to compute other parameters like the size of the object or its shape. On the computer processing part, orbit calculation could be performed. This would allow prediction of paths free of objects (for space launches for example).

REFERENCES

[1] Christophe BONNAL, *Détection des débris spatiaux et catalogage* [Internet]. https://www.universalis.fr/encyclopedie/debris-spatiaux/2-detection-des-debris-spatiaux-et-catalogage/

[2] Wikipedia, *GRAVES (systeme)* [Internet]. https://fr.wikipedia.org/wiki/GRAVES_(systeme)

[3] Hervé Lamy, *What is BRAMS?* [Internet]. https://brams.aeronomie.be

[4] Michal Th., Euglizeaud J.P. and Bouchard.J *Radar VHF et émission d'amateur* [Internet]. https://adsabs.harvard.edu/full/2005ESASP.587...61M

[5] Wikipedia, *Très haute fréquence* [Internet]. https://fr.wikipedia.org/wiki/Tres_haute_frequence

[6] F6CRP team, *Radar VHF et émission d'amateur* [Internet]. https://f6crp.pagesperso-orange.fr/ba/graves.htm

[7] Société astronomique de touraine, *RADIOASTRONOMIE : LES OREILLES DU CIEL* [Internet]. https://www.astrotouraine.fr/radioastronomie-les-oreilles-du-ciel/

[8] Allen Thomson, *A GRAVES Sourcebook* [Internet]. https://spp.fas.org/military/program/track/graves.pdf

[9] Vigie Ciel, *Le projet fripon* [Internet]. https://www.vigie-ciel.org/le-projet-fripon/

[10] Distance fr team, *Distance entre Dijon et Lausanne* [Internet]. https://fr.distance.to/Dijon/Lausanne

[11] Passion radio team, *Antenne Base VHF 140-160 MHz Yagi 3 et 4 éléments Sirio WY140 3N & 4N* [Internet]. https://www.passion-radio.fr/fixe/wy1403n-1130.html

[12] Passion radio, *Dongle FUNcube Pro+ Plus* [Internet]. https://www.passion-radio.fr/cles-rtl-sdr/funcube-dongle-pro-72.html

[13] Cédric Willemin, *Détection de Météores et d'Aéronefs* [Internet]. https://www.willemin.li/cedric/documents/radar/Willemin_TM2019_Document.pdf/

[14] Faber Acoustical, *SignalScope Pro 2020* [Internet]. https://www.faberacoustical.com/apps/signalscope/signalscope_pro_2020/

[15] Cédric Willemin, *Détection de Météores et d'Aéronefs* [Internet]. https://sjf.ch/detection-de-meteores-et-daeronefs/

[16] Kohei Yamamoto, Koji Endo and Tomoaki Ohtsuki, *Remote Sensing of Heartbeat based on Space Diversity Using MIMO FMCW Radar* [Internet]. https://ieeexplore.ieee.org/stamp/stamp.jsp?tp=&arnumber=9685033

[17] Casademont, Titus and Hort, Matthias and Scharff, Lea and Peters, Gerhard, *I-Channel FMCW Doppler Radar for Long-Range and High-Velocity Targets* [Internet]. https://ieeexplore.ieee.org/document/9430893

[18] Nizar Bouhlel, Stéphane Meric, Claude Moullec and Christian Brousseau, *Système radar FMCW pour l'identification de transpondeurs* [Internet]. https://hal.archives-ouvertes.fr/hal-01894273/document

[19] Le campus numérique des iut, *Phase et fréquence* [Internet]. https://public.iutenligne.net/electronique/launay/modulation_analogique/chap3/3-1-c.html

[20] O. Başarslan and E. Yaldız, *Implementation of FMCW radar for training applications* [Internet]. https://ieeexplore.ieee.org/document/7935839

[21] Wikipedia, *S band* [Internet]. https://en.wikipedia.org/wiki/S_band

[22] Orange, *REPARTITIONS ET UTILISATIONS DES FREQUENCES RADIOAMATEURS* [Internet]. https://radio.pagesperso-orange.fr/FreqRA.htm#24G

[23] Wikipedia, *Costas loop* [Internet]. https://en.wikipedia.org/wiki/Costas_loop

[24] Simon Henault, Jean-Francois Guimond, *Orbit estimation using passive radio frequency observations* [Internet]. https://cradpdf.drdc-rddc.gc.ca/PDFS/unc361/p813190_A1b.pdf

[25] Christian Wolff, *Angular Resolution* [Internet]. https://www.radartutorial.eu/01.basics/Angular%20Resolution.en.html

[26] String fixer, *Résolution angulaire* [Internet]. https://stringfixer.com/fr/Rayleigh_criterion

[27] Zeeshan, *Uniform Linear Array (ULA) beamwidth and angular resolution using FFT* [Internet]. https://electronics.stackexchange.com/questions/288530/uniform-linear-array-ula-beamwidth-and-angular-resolution-using-fft

[28] Sulimov, Amir I. and Karpov, Arkadiy V, *Simulation of Frequency-Selective Properties of Meteor Scatter Radio Links* [Internet]. https://ieeexplore.ieee.org/stamp/stamp.jsp?tp=&arnumber=8810184

[29] Ramin Deban, *Analyse et développement de radar à diversité spatiale: applications à l'évitement de collisions de véhicules et au positionnement local* [Internet]. https://publications.polymtl.ca/281/1/2010_RaminDeban.pdf

[30] George Hardesty, *Antenna radiation patterns : H-plane, E-plane, XY,XZ and YZ planes* [Internet]. https://www.data-alliance.net/blog/antenna-radiation-patterns-hplane-eplane-xy-xz-yz-planes/

[31] Hervé Choplin et le Groupe Radio-Astronomie, *Détection, observation des radio-météores* [Internet]. https://media.afastronomie.fr/RCE/PresentationsRCE2018/Choplin-RCE2018.pdf